Optical properties of some glassy compositions of the $GeSe_{2-x}Sn_x$ thin films of the ternary chalcogenide system

R. Khadour[(1)], F. Saiouf[(2)], I. Mdawar[(3)]

Received 14/05/2014
Accepted 23/09/2014

ABSTRACT

The optical transmission T(λ) spectra has been recorded, in the spectral range of 400-1100 nm, for thermally evaporated Sn doped $GeSe_{2-x}Sn_x$ films. The X- ray diffraction technique was used to confirm the polymeric nature of the studied films. The current optical theories and models were applied to analyze the recorded spectra and to calculate various interesting optical parameters. These include: dispersion of the two components of both complex refractive index ($\hat{n}$=n-ik) and complex dielectric constant (ε_1 and ε_2), energy gap (E_g), Urbach energy (E_u), single oscillator energy (E_o), lattice oscillating strength (E_d). At this point, a similar non-monotonic trend is observed for the compositional dependence of various parameters. This has been ascribed to the disorder and/or structural defects introduced due to the incorporation of Sn, up to 33.34 % Sn, in the $GeSe_{2-x}Sn_x$ structure.

It is observed that band gap decreases with the increase of Sn concentration in the system. This variation in the band gap is explained on the basis of change in structure of the system due to the introduction of Sn in Ge-Se-Sn glassy system.

Keywords: Chalcogenide glass, Thin films, Optical band gap, Transmission, Urbach energy, Complex dielectric constant, Absorption coefficient.

[(1)] Ph., D. Student, [(3)] Assistant Prof., Department of Physics, Faculty of Sciences, University of Damascus, Syria.
[(2)] Prof., High In Stitute of Laser Research and Application.

الخواص الضوئية لأفلام رقيقة لبعض التركيبات الزجاجية للنظام الشالكوجيني ثلاثي الطور $GeSe_{2-x}Sn_x$

رائد خضور[1] و فواز سيوف[2] و إياد مدور[3]

تاريخ الإيداع 2014/05/14

قبل للنشر في 2014/09/23

الملخص

سُجّل طيف النفوذية T(λ) في المجال الطيفي 400-1100 nm لأفلامٍ رقيقة من النمط $GeSe_{2-x}Sn_x$ المحضرة بطريقة التبخير الحراري. ومن ثمّ جرى التأكد من الطبيعة البوليميرية للأفلام المدروسة، باستخدام تقنية انعراج الأشعة السينية، وكذلك تحليل بيانات طيف النفوذية المسجل بالاعتماد على النماذج والنظريات الحديثة، وذلك بهدف حساب العديد من المتحولات الضوئية التي تتضمن: تشتت مركبتي قرينة الانكسار العقدية (n=n-ik^)، وثابت العزل الكهربائي (ε_1 and ε_2)، وعرض الفجوة الطاقية (E_g)، وطاقة ايربخ (E_u)، وطاقة المذبذب الأحادي (E_o)، وقوة التذبذب الشبكي (E_d). واعتماداً على ما سبق لوحظ ارتباط غير مطرد لقيم هذه المتحولات بتركيب تلك العينات، وفسر هذا بسبب العشوائية و/ أو العيوب البنيوية الناتجة من دخول عنصر القصدير بنسبة أكثر من 33.34% في بنية النمط $GeSe_{2-x}Sn_x$.

لوحظ أن الفجوة الطاقية (E_g) تتناقص بزيادة تركيز عنصر القصدير Sn في المنظومة المدروسة، وهذا التغير في عرض الفجوة الطاقية يفسر أيضاً نتيجة للتغير في البنية الزجاجية للمنظومة $GeSe_{2-x}Sn_x$ بسبب دخول القصدير فيها.

الكلمات المفتاحية: زجاج شالكوجيني، فلم رقيق، الفجوة الطاقية الضوئية، النفوذية، طاقة ايربخ، ثابت العزل، معامل الامتصاص.

[1] طالب دكتوراه، [3] مدّرس، قسم الفيزياء، كلية العلوم، جامعة دمشق، سورية.

[2] أستاذ، المعهد العالي لبحوث الليزر وتطبيقاته.

1. Introduction

Chalcogenide glasses (ChG's) with their flexible structure, enormous variation in properties, and almost unlimited ability for doping and alloying are promising candidates for photonic applications due to their attractive optical properties, such as high refractive index, high photosensitivity and large optical nonlinearity. The investigation of the optical properties of ChG's is of considerable interest and affords critical information about the electronic band structure, optical transitions and relaxation mechanisms. The optical and electrical properties of ChG's are generally much less sensitive to non-stoichiometry and the presence of impurities is less sensitive than crystalline semiconductors. Moreover, ChG's are conducive for use in fiber optics and integrated optics since they have many unique optical properties and exhibit a good transparency in the infrared region,[1,2]. Because of their IR transparency, photosensitivity, high optical nonlinearity, and rare-earth doping potential, these glasses have been utilized to fabricate photonic devices such as fibers, [3] planar waveguides,[4,5] gratings, all-optical switches, and fiber amplifiers.

Device applications using ChG's usually require the glass to be processed into either fiber or thin film form. The wide practical application of thin amorphous chalcogenide films, especially Se-glasses on the basis of Ge, is closely connected with their good transparency in the visible and IR spectral regions and with the possibility to create optical media with defined values of the refractive index, dispersion, and extinction coefficients. The relatively low energy of the chemical bonds in the Ge-based ChG's offers the opportunity for photostructural transformations and a number of other light-induced effects, all of which are typically accompanied by considerable changes in the chalcogenide's optical constants,[6].

2. Theoretical background

2.1) Optical absorption spectroscopy of amorphous semiconductors.

In amorphous semiconductors, the optical absorption edge spectra generally contain three distinct region [7]:

a) **High absorption region** ($\alpha \geq 10^4$ cm^{-1}), which involves the optical transition between valence band and conduction band which determines the optical band gap. The absorption coefficient in this region is given by:

$$\alpha(h\nu) = B\left(h\nu - E_g\right)^P$$

where E_g is the optical band gap and B is a constant related to band tailing parameter. In the above equation, p=1/2 for a direct allowed transition = 3/2 for a direct forbidden transition, p=2 for an indirect allowed transition and p=3 for an indirect forbidden transition.

b) **Spectral region with** ($10^2 \geq \alpha \geq 10^4$ cm^{-1}) is called Urbach's exponential tail region in which absorption depends exponentially on photon energy [8]and is given by:

$$\alpha(h\nu) = \alpha_0 exp\left(\frac{h\nu}{E_u}\right)$$

Where α_0 is a constant and E_u is interpreted as band tailing width of localized states, where the absorption in this region is due to transitions between extended states in one of the bands and localized states in the exponential tail of the other band [9]. The inverse slope, or the width of the exponential edge (E_u), reflects the width of the more extended band tail that is often called Urbach energy. Such exponential, or Urbach, edge is usually ascribed to localized states at the band edges. In other words, the Urbach edge is determined by the degree of disorder (e.g., charged impurities) and/or structural defects (e.g., broken or dangling bonds, vacancies, non-bridging atoms, or chain ends) in the considered semiconductor material [10]. The structural defects are collected together or assembled with impurities thus forming defect complexes in order to obtain a lower energy state.

c) **The region with** ($\alpha \geq 10^2$ cm^{-1}) involves low energy absorption and originates from defects and impurities.

3. Experimental procedure

Homogeneous massive bulk ingots (5gr) of $GeSe_{2-x}Sn_x$ (where x = 0, 0.2, 0.4, 0.6, 0.8 &1) glassy materials were prepared by melt

quenching technique[11]. The high purity constituent materials were taken in elemental powders form. Mixture of these powders was then sealed in a quartz ampoule and this ampoule was heated at a maximum temperature about 950 Cº for 12 hours. The ampoule was frequently shaken to achieve better homogeneity. Finally the heated ampoule was quenched in ice-cooled water. To avoid fracture of the tube and glass ingot, and to minimize inner tension induced by a quenching step the ampoules were subsequently returned to the furnace for annealing for 5 h at 40 C° below the glass transition temperature T_g. So obtained ingot of material was grinded into its powder form. These powders were then used to deposit films using thermal evaporation technique under a starting pressure of 10^{-5} Torr on glass substrates (the substrate temperature ≈ 250 C^0, rate of deposition ≈ 7-10 $A^o.s^{-1}$, The thickness of thin films ≈ 400 nm). The films were kept inside the deposition chamber for 10 hours to achieve the metastable equilibrium. The nature of the structural phase of the as-prepared films were confirmed using an X-ray diffraction (XRD) computerized system (model: Ital products ADP 200 diffractometer) with Cu, Kα radiation of wavelength λ= 0.15406 nm, Fig(1). Measurements of the transmittance T(λ) were carried out using a computer-aided UV–VIS–NIR spectrophotometer (type: OPTIZEN 2120UV PLUS). The function T=f(λ) was recorded at normal incidence. A resolution limit of 0.3 nm and a sampling interval of 1 nm are utilized for the different measuring points. Also, the accuracy of measuring T(λ) is 0.004. The measurements were carried out at RT for the recorded entire spectral range of 300–1100 nm.

4. Results and discussion

4.1. Nature of as-deposited films

The XRD pattern shown in Fig(1) reveal the amorphous nature of $GeSe_{2-x}Sn_x$ films. Since no peaks were observed in the XRD pattern.

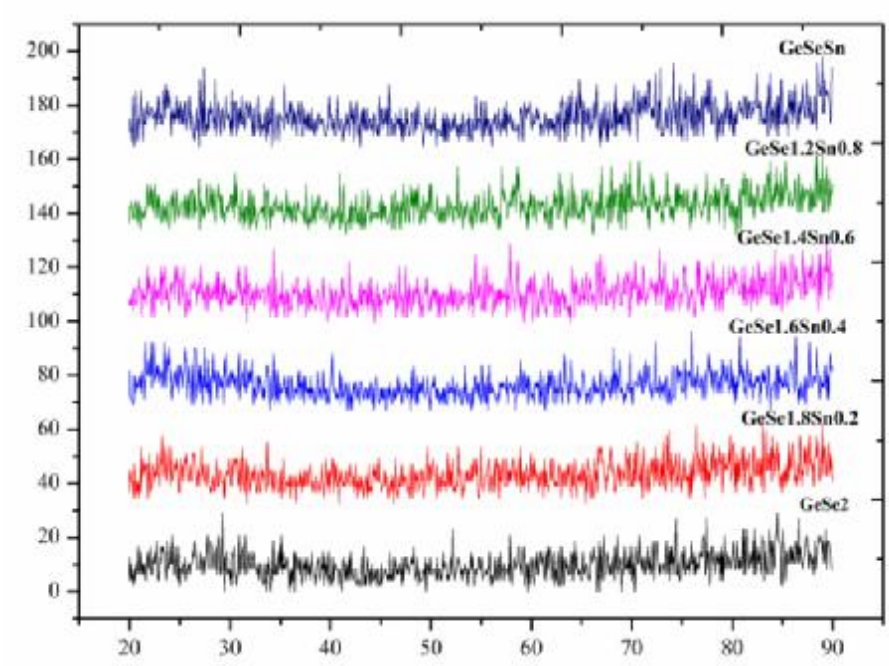

Fig. 1. XRD pattern of $GeSe_{2-x}Sn_x$ glassy film. (where x = 0, 0.2, 0.4, 0.6,0.8 &1).

4.2. Transmission spectra.

The transmission spectra in the wavelength range 300–1100 nm at normal incidence of the as-evaporated $GeSe_{2-x}Sn_x$ thin films are shown respectively in Fig(2). The averages of the transmission values of all the layers in the transparency region (800 - 1100 nm) are 60 % and 97 % respectively.

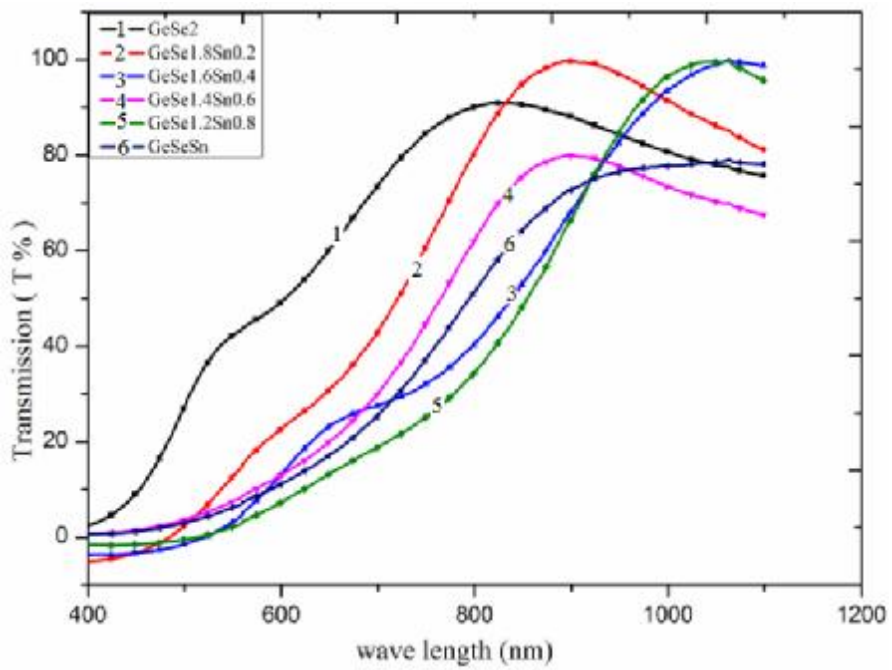

Fig. 2. Transmittance versus wavelength as recorded for the studied $GeSe_{2-x}Sn_x$ films.

4.3. Determination of optical constants

4.3.1. Short-wavelength absorption

Fig(3) shows the dependence of short-wavelength absorption edge $GeSe_{2-x}Sn_x$ system. The short-wavelength absorption edge shifts to the longer wavelength with the addition of Sn content which is induced by two factors. First, it is due to the decreasing relatively strong Ge-Se bonds (49.5 kcal/mol) And the increasing weak Ge-Sn bonds (37.4 kcal/mol). Second, the addition of tin will generally decrease the optical band gap (E_g) [25-27], These two factors result in a red-shift of the short-wave absorption edge.

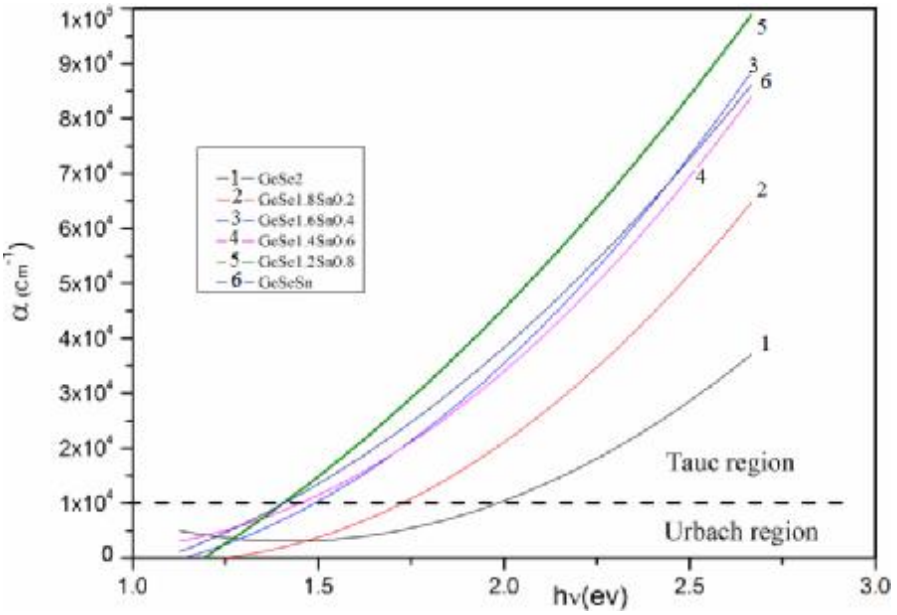

Fig. 3. The calculated absorption coefficient as a function of photon energy in the Tauc and Urbach regions for the investigated films.

4.3.2. Optical band gap

Plot of the function α=f (hυ) for each investigated composition that shown in Fig. 4, could be subdivided into two regions :

- The first region is for the higher values of the absorption coefficient, namely for $\alpha(h\nu) > 10^4$ cm^{-1}, that corresponds to transitions among extended states in both valence and conduction bands. The functional dependence of the optical absorption coefficient $(\alpha h\nu)^{1/2}$ versus hν is shown in Fig (4) for the investigated films. For each composition, the energy gap (E_g) has been calculated by fitting the straight part in the high energy region of the function $(\alpha h\nu)^{1/2} = f(h\nu)$, locally point by point, to a linear regression line with fitting parameter $R_2 \approx 0.99$ and the results are given in Table 1. At this point, the value of E_g shows a decrease from 2.149±0.013 (This value is in good agreement with previously reported data [24]) to 1.973±0.011 eV with the introduction of 33.34 % Sn into $GeSe_2$.

The decrease in optical band gap may be explained on the basis of the average bond energies of the system. Pauling proposed [13] that single covalent bond energy of heteroatomic bonds D(A-B) can be estimated from the single covalent bond energy of homoatomic bonds D(A-A) and D(B-B) and the electronegativity, χ_A of atom A and χ_B of atom B using the formula:

$$D(A-B) = [D(A-A)D(B-B)]^{1/2} + 30(c_A - c_B)^2$$

The $D(A-A)$ values used are in units of kcal/mol 37.6 for Ge, 44 for Se and 34.2 for Sn, the χ values of the atoms involved are 2.01 for Ge, 2.55 for Se and 1.96 for Sn. The introduction of Sn atoms in the system $GeSe_{2-x}Sn_x$ is accompanied by the replacement of Se atoms by Sn atoms forming Ge-Sn bonds, thus decreasing the concentration of Ge-Se and Se-Se bonds. Since the bond energy of Ge-Sn bonds (37.4 kcal/mol) is lower than that of the Ge-Se (49.5 kcal/mol) bonds, the average bond energy of the system decreases, which results in the reduction in the optical band gap. The relationships between optical gap and content of Sn are illustrated in the upper left insert Fig(4).

- The second region for α(hν) is for the lower values of α, that is for α (hν) < 10^4 cm^{-1}, where the absorption in this region is due to transitions between extended states in one of the bands and localized states in the exponential tail of the other band. The inverse slope, or the width of the exponential edge (E_u), reflects the width of the more extended band tail that is often called Urbach energy. The calculated values of E_u are given in Table 1 as a function of film composition. These values show an increase at the first addition of Sn content with a small concentration around 6.67% in $GeSe_{1.8}Sn_{0.2}$ sample and then the increasing addition of the Sn content at the expense of Se content decreases the E_u values. It is interesting to note that; a limited addition of Sn content (from 0 to 6.67 At %) increases the E_u values (from 0.183 to 0.199 eV). Such decrease in the E_u indicates an increase in the disorder character of $GeSe_2$ due to the introduction of *Sn*. This may be due to the formation of charged impurities and/or structural defects in the quasi-gap of $GeSe_{1.8}Sn_{0.2}$ than do in that of $GeSe_2$.This may mean that, the *Sn* atoms [of atomic radii = 1.62 A^0] will introduce

to the lattice sites of the parent sample $GeSe_2$, which will produce a non-bridging bond that will disturb the equilibrium of the structure. This might cause a distribution in lattice positions of the other atoms Ge and Se. This in turn goes to more structural disorder in the sample. Also, the fact that $GeSe_{1.8}Sn_{0.2}$ (2.103±0.017 eV) has smaller energy gap than $GeSe_2$ (2.149±0.018 eV), implies that the formation of defects in the narrower gap will have more effect [14,15]. Conversely, the increasing addition of Sn content (from 6.67 to 33.34 At %) leads to decreasing the width of the localized tail states to 0.153 eV. Such a decrease of *Eu* is attributed to the crystallized character of the thermally evaporated film.). This may mean that, the Sn atom concentration should be enough to that the system should regard Sn atoms as heterogeneous nucleation sites. This leads to make the crystallization procedure a more desirable choice, which justifies the slope decrease in the E_u values. Also, the presence of band tail (E_u) that accompanied the localized states in the gap reflects some degree of disorder in the considered semiconductor film.

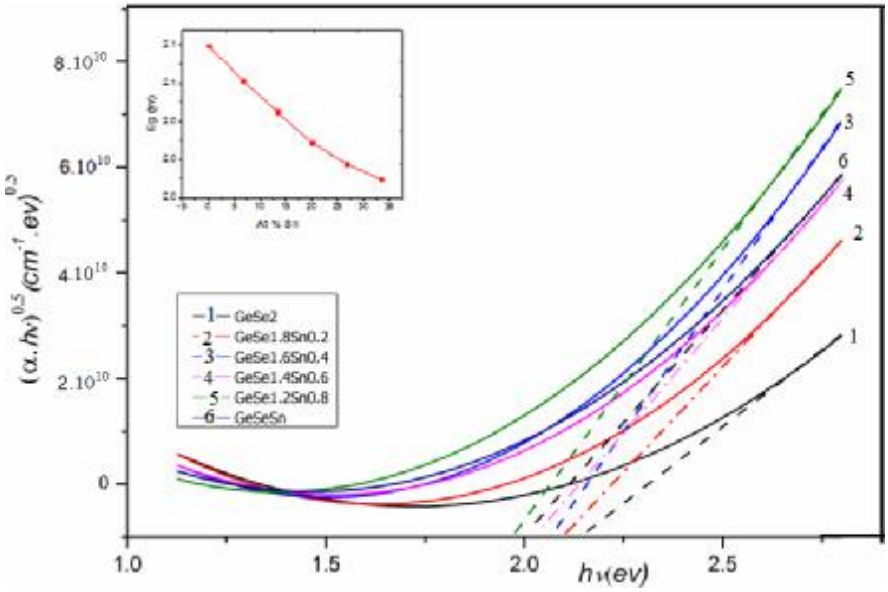

Fig. 4. Tauk's plots for determining the optical energy gap of indirect transitions for the investigated films.

Table 1. The indirect optical energy gap (E_g), Urbach energy (E_u), The single oscillator energy (E_o), dispersion energy (E_d)

Film Composition	E_g (eV)	E_u (eV)	E_0(eV)	E_d(eV)
$GeSe_2$	2.149	0.183	4.577	22.341
$GeSe_{1.8}Sn_{0.2}$	2.103	0.199	3.571	11.565
$GeSe_{1.6}Sn_{0.4}$	2.062	0.169	3.982	15.485
$GeSe_{1.4}Sn_{0.6}$	2.021	0.161	3.765	12.245
$GeSe_{1.2}Sn_{0.8}$	1.994	0.155	3.712	12.823
$GeSeSn$	1.973	0.153	3.621	13.457

4.3.3. Average energy gap and dispersion energy from WDD model

According to the single oscillator model proposed by Wemple and DiDomenico [16] the optical data could be described to a very good approximately by the following formula:

$$n^2 - 1 = \frac{E_o E_d}{E_o^2 - (h\nu)^2}$$

where, n is the refractive index, E_0 is the average oscillator energy gap, and E_d is the so-called dispersion energy. The latter quantity measures the average strength of the inter-band optical transitions. Plotting $(n^2 - 1)^{-1}$ against $(h\nu)^2$ allows the determination of the oscillator parameters by fitting a straight line to the points. The value of E_0 and E_d can be directly determined from the slope $(E_0.E_d)^{-1}$ and the intercept on the vertical axis, (E_d/E_0). The values obtained for the dispersion parameters, E_0 and E_d are tabulated in Table 1. As was found by Tanaka [17], the first approximate value of the optical band gap, E_g, is also derived from the Wemple – DiDomenico dispersion relationship, according to the expression $E_g \approx E_0/2$. The values so obtained from this equation are in almost agreement with the values obtained from the Tauc's extrapolation using the value of the absorption coefficient from the T and R measurements.

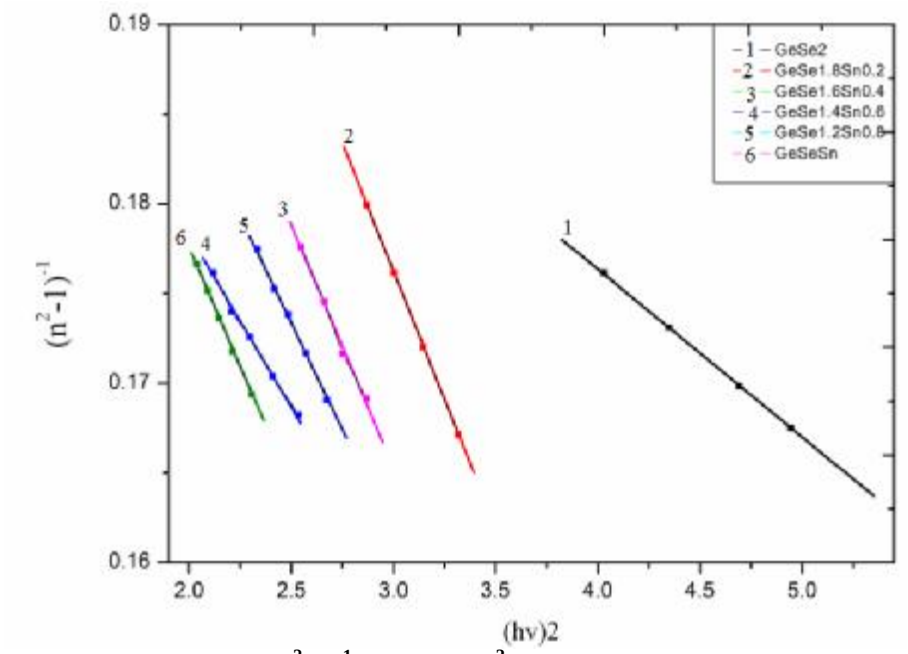

Fig. 5. Plots of $(n^2-1)^{-1}$ versus $(hv)^2$ for the investigated films.

4.3.4. Refractive Index

The wavelength dependence on the refractive index has been calculated in the range between 200nm to 1100 nm on the $GeSe_{2-x}Sn_x$ films. Using the equations :

$$n = [4R/(R-1)^2 - k^2]^{1/2} - (R + 1)/(R - 1)$$

where R is the reflectance [19], k is the extinction coefficient. Fig.6 shows the variation of refractive index with wavelength of $GeSe_{2-x}Sn_x$ films for different values of composition. It is found from this Figure that the refractive index decreases with the increasing of wavelength of the incident photon. And we can observed the appearance of a peak occurring in dispersion of the refractive index of the films, this was attributed to the rapid change in the optical absorption coefficient in the vicinity of the absorption edge [18, 19].

4.3.5. Extinction Coefficient

The relation between the extinction coefficient (k) (which is calculated from the relation: $k = \alpha.\lambda/4\pi$) and wavelength for $GeSe_{2-x}Sn_x$ films is shown in Fig. 7. From this Figure it is found that the extinction coefficient takes the similar behavior of the corresponding absorption coefficient. One can deduce from this figure that the extinction coefficient decreased with increasing the wavelength up to ≈ 760 nm due to the high values of the absorption coefficient at this range of wavelength. The extinction coefficients values are similar to that of the absorption coefficients for the same reasons as mentioned before. Our results are in agreement with the results found by Pan *et al.*, [20] and by Sharma *et al.*, [21].

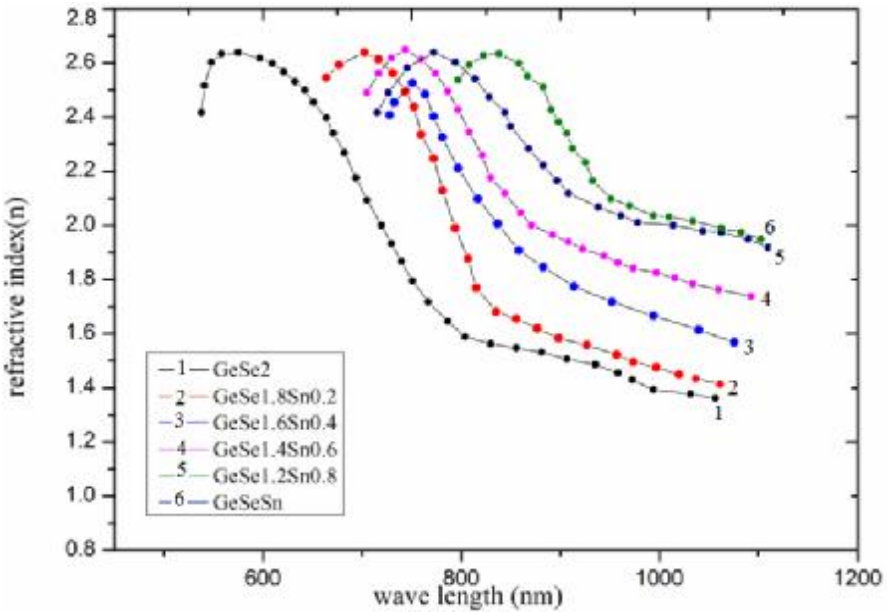

Fig. 6. Plots of the fitted refractive index versus wavelength for the investigated films.

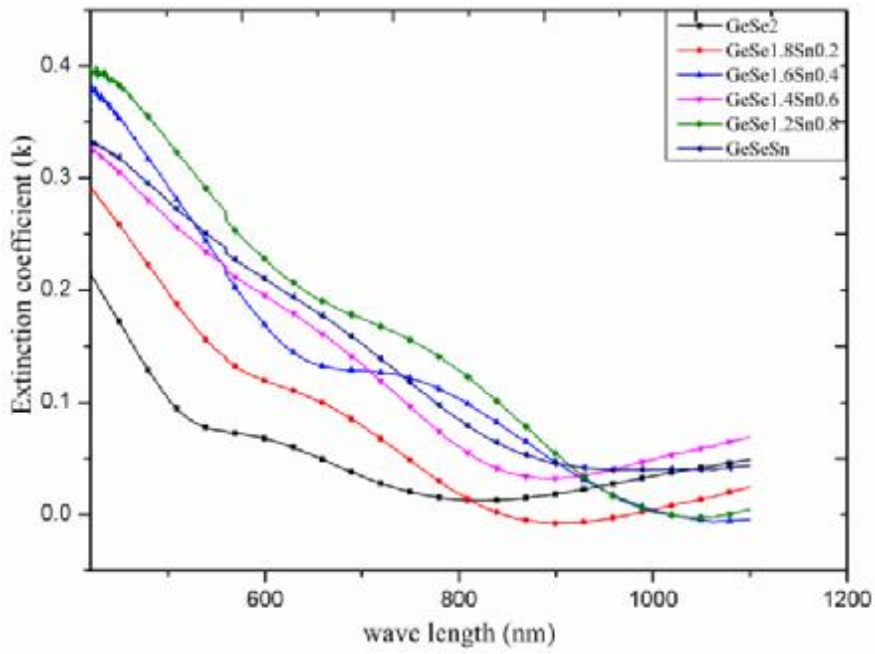

Fig. 7. The extinction coefficient with wave length for $GeSe_{2-x}Sn_x$ film at different composition.

4.3.6. dielectric constant

The Real ε_1 and Imaginary ε_2 Parts Coefficient Figs. 8a and 8b show the variation of the real (ε_1, which is calculated from the relation, $\varepsilon_1 = n_2 - k_2$ [21,23]) and imaginary (ε_2, which is calculated from the relation $\varepsilon_2 = 2nk$) parts of the dielectric constant with the wavelength for $GeSe_{2-x}Sn_x$ films. The behaviors of ε_1 and ε_2 are the same as those of n and k, respectively with the variation of x values. This is due to that the variations of ε_1 mainly depends on the value of n_2, because of the smaller values of k_2 comparison with (n_2, while the imaginary part of the dielectric constant mainly depends on k values which were related to the variations of absorption coefficient.

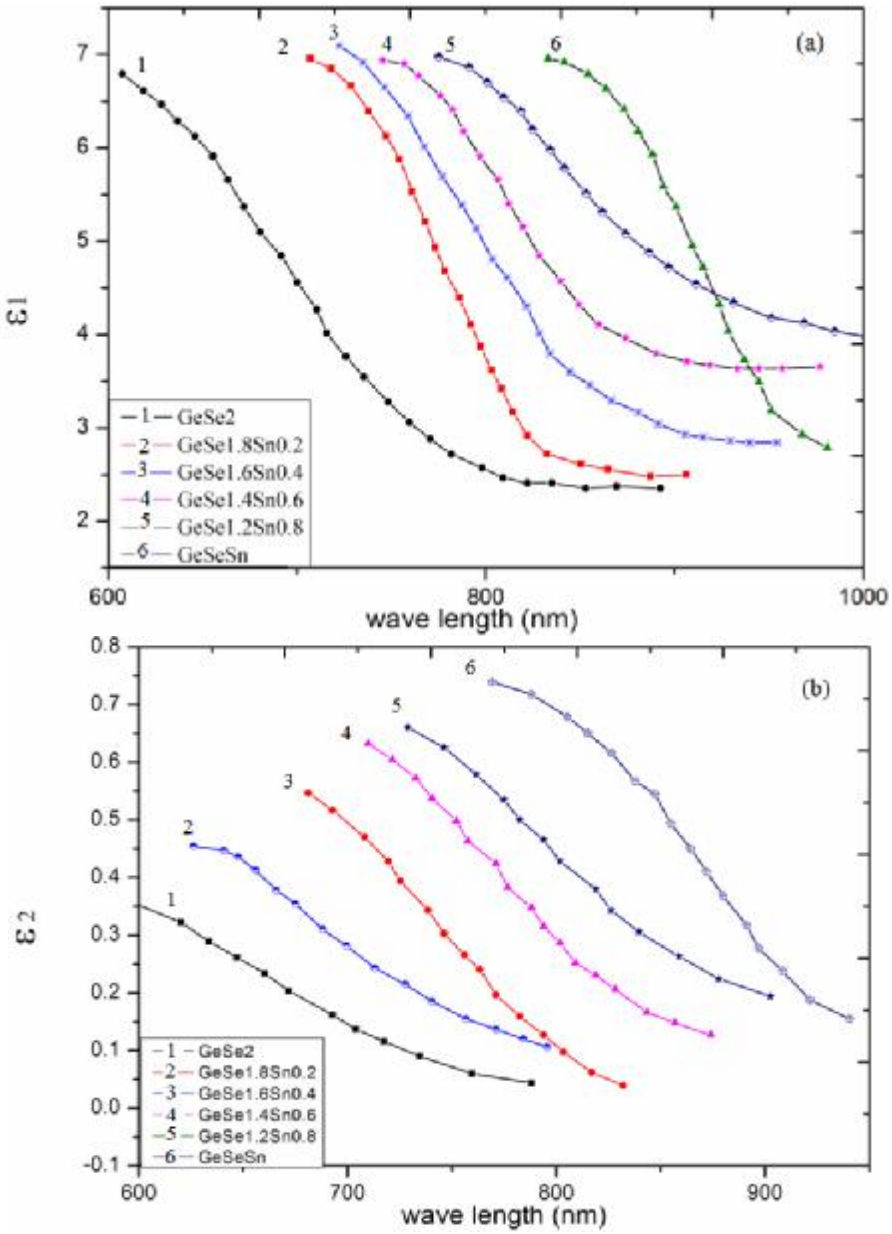

Fig. 8. (a) The real & (b) imaginary part of dielectric constant as a function of wavelength $GeSe_{2-x}Sn_x$ thin films.

4.4. Infrared optical transmission

Fig.9 shows the optical transmission spectra of $GeSe_{2-x}Sn_x$ glassy samples. It is seen from Fig. 9 that few absorption bands occur in the IR spectra due to highly pure *Ge* and *Se* elements in our experiments, which means that the impurities in the $GeSe_{2-x}Sn_x$ film are few. (4.12μm) absorption band are observed in the IR spectra according to Se-H impurity [24]. The transmission of the studied glassy samples extends in the MIR with a cut-off edge beyond 5 μm, it is assigned to the intrinsic multiphonon vibrations of Ge-Se. The transmission rate of the $GeSe_{2-x}Sn_x$ glassy samples decrease with increase the *Sn* content, which could be explained by the following two factors. One is owing to more Fresbel's losses with increasing content of Sn, because Fresnel's losses depend on the refractive index, and the increasing content of *Sn* leads to a shift in the higher refractive index forward the IR region. Another is due to the enhanced crystal-forming ability in the presence of the increasing content of *Sn*, which leads to the increase of scattering loss of glasses.

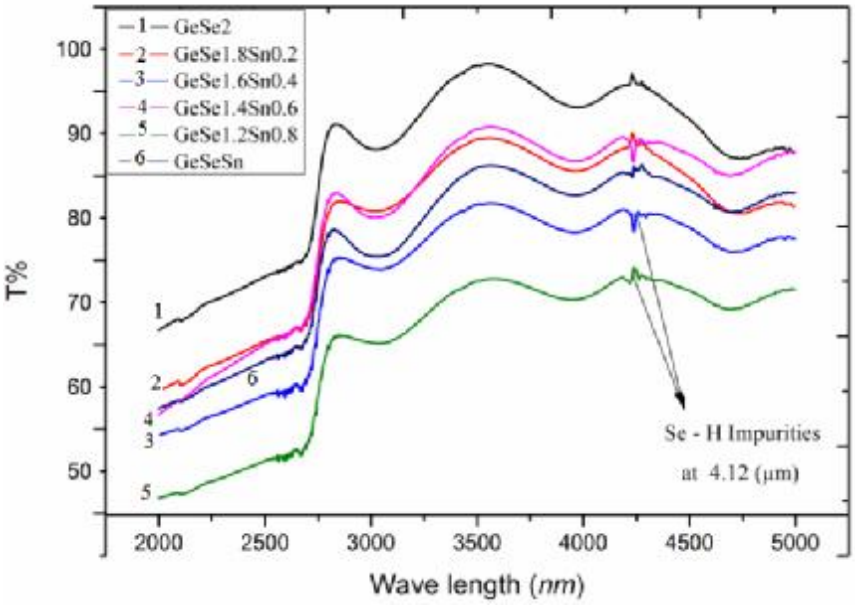

Fig. 9. The IR transmission spectra $GeSe_{2-x}Sn_x$ thin films

5. CONCLUSIONS

The optical properties of $GeSe_{2-x}Sn_x$ (where x= 0, 0.2, 0.4, 0.6, 0.8 &1) thin films have been measured and calculated from the transmission spectra. An extensive investigation for the increasing addition of Sn, applying the current optical theories and models on the recorded T(λ) spectra, bringing about the subsequent remarks:

- A non-monotonic trend, whether towards lower or higher wave-lengths, for the Sn-increasing concentration of the two components of the complex dielectric constant (ε_1 and ε_2), dispersion refractive index (n), optical energy gap of indirect transitions (E_g), Urbach energy (E_u), lattice oscillating strength (E_d) as well as for the single oscillator energy (E_o).
- The glassy material has high value of refractive index and decreasing optical band gap with increasing content of Sn in the glassy matrix.
- There is a good consistency which has been found between the results obtained in the present work and those previously reported by other authors for related alloys.
- Incorporation of Sn into the $GeSe_{2-x}Sn_x$ host matrix introduces new Ge-Sn chemical bonds, with smaller binding energy than that of the Ge-Se bonds, which explains the increase of n, and decrease of the Tauc gap.
- Lastly, the change in the refractive index after the addition of Sn content, and increase Urbach energy (E_u) for the $GeSe_{1.8}Sn_{0.2}$ sample makes it, an attractive candidate as optical recording medium.

.

References

[1] Zakery. A. and Elliott. S. R. (2003). "Optical properties and applications of chalcogenide glasses: a review," ***J. Non-Cryst. Solids*** **330(1-3): 1–12.**

[2] Sanghera J. S. and Aggarwal. I. D. (1999). "Active and passive chalcogenide glass optical fibers for IR applications: a review" ***J. Non-Cryst. Solids.*** **256-257, 6–16.**

[3] Tanaka K. (2005). "Optical nonlinearity in photonic glasses," ***J. Mater. Sci. Mater. Electron.*** **16(10): 633–643.**

[4] Viens. J., Meneghini. C., Villeneuve. A., Galstian. T., Knystautas. E., Duguay. M., Richardson. K. and Cardinal. T. (1999). "Fabrication and characterization of integrated optical waveguides in sulfide chalcogenide glasses" ***J. Lightwave Technol.*** **17, 1184.**

[5] Ruan. Y., Li. W., Jarvis. R., Madsen. N., Rode. A. and Luther-Davies. B. (2004). "Fabrication and characterization of low loss rib chalcogenide waveguides made by dry etching" ***Opt. Express.*** **12: 5140-5145.**

[6] Galstyan. T., Viens. J., Villeneuve. A., Richardson. K. and Duguay. M. (1997). "Photoinduced self-developing relief gratings in thin film chalcogenide As2S3 glasses" ***J. Lightwave Technol.*** **15: 1343-1347.**

[7] Elliot. S.R. (1990). "Physics of Amorphous Materials", ***Essex: Longman Group Limited,*** **New York .**

[8] Franz Urbach. (1953). "The Long-Wavelength Edge of Photographic Sensitivity and of the Electronic Absorption of Solids" ***Physical Review.*** **92: 1324–1324.**

[9] Cohen. M. H., Soukoulis. C. M., Economou. E. N., Taylor. P.C. and Bishop. S. Eds. (1984). "Optical Effects in Amorphous Semiconductors" ***AIP ConJ Proc.*** **120, 371.**

[10] Mott. N.F., Davis. E.A. (1979). "Electronic Processes in Non-Crystalline Materials" ***Clarendon Press,*** **Oxford.**

[11] Wei Lu and Charles. M. L. (2006). "Semiconductor nanowires" ***J.Phys.*** **D:** ***Appl.phys.*** **39, 190.**

[12] Swanepoel. R. (1983). "Determination of the thickness and optical constants of amorphous silicon" ***J. Phys. E. Sci. Instrum.*** **16: 1214–1222.**

[13] Pauling. L. (1960). "The Nature of the Chemical Bond" (3rd Edition), ***Cornell University Press,*** **Ithaca, NY.**

[14] El-Fouly. M.H., Kotkata. M.F., El-Behay. A.Z., Morsy. M.A., Radiat. (1984). "Doping effect of Sm on the enerrey GAP and optical dipersion of a-Se " ***Phys. Chem.*** **7 (3): 145- 157.**

[15] Kotkata. M.F., El-Fouly. M.H., Fayek. S.A., El-Hakim. S.A. (1986). "The effect of Tl addition on the electrical and thermal transport properties of amorphous As2Se3" ***Semicond. Sci. Technol.*** **1 313.**

[16] Wemple. S. H. and DiDomenico. M. (1971). "Behavior of electronic dielectric constant in covalent and ionic materials" ***Phys. Rev.*** **B 3(4): 1338–1351.**

[17] Zakery. A. and Elliott. S. R. (2003). "Optical properties and applications of chalcogenide glasses: a review," ***J. Non-Cryst. Solids.*** **330 (1-3): 1–12.**

[18] Sharma. P., Vashistha. M., Jain. I. P. (2005). "Optical properties of Ge20Se80-xBix thin films" ***Journal of Optoelectronics and Advanced Materials*****. 7 (5): 2647-2654.**

[19] Sharma. I., Tripathiand. S.K., Barman. P.B. (2008). "Effect of Bi addition on the optical behavior of a-Ge–Se–In–Bi thin films" ***Applied Surface Science.*** **255: 2791-2795.**

[20] Pan. R.K., Tao. H.Z., Zang. H.C., Zhao. X.J., Zhang. T.J. (2010). "Optical properties of pulsed laser deposited amorphous (GeSe2)100−*x* –Bi *x* films" ***Applied Physics*****, 99: 889-894.**

[21] Tohge. N., Minami. T., Tanaka. M. (1980). "Electrical and optical properties of n-type semiconducting chalcogenide glasses in the system Ge-Bi-Se" ***J. Appl. Phys*****. 51 (2).**

[22] Chadhriand. S., Biswon. S. (1981). "Amorphous to crystalline transition of selenium thin films of different thicknesses" ***J. Non. Cryst. Solid*** **4:171.**

[23] Reitter. A. M., Sreeram. A. N., Varshneya. A. K., Suiler. D. R. (1992). "Modified Preparation Procedure for Laboratory Melting of Multicomponent Chalcogenide Glasses" ***J. Non-Cryst. Solids*****.139: 121.**

[24] Thakur. A., Sharma. V., Saini. G.S.S., Goyaln., Tripathis .K. (2005). "Calculation of optical parameters of a-Ge-Se-Sn thin films" ***Journal of Optoelectronics and Advanced Materials.*** **7(4: 2077–2083.**

[25] Vibhav. K., Saraswat. V., Kishore, D., Kananbala Sharma.N.S., Saxena. T P., Sharma. (2007). "Band gap studies on Se-Te-Sn ternary glassy films Chalcogenide Letters". 4(5): 61 – 64.

[26] VivekModgil. and Rangra. V. S. (2014). "Effect of Sn Addition on Thermal and Optical Properties of Glass Pb9Se71Ge20-xSnx" Hindawi Publishing Corporation, ***Journal of Materials*****.,Article ID 318262 8 pages.**

[27] McNeil. L. E., Mikrut. J. M. and Peters. M. J. (1992). "Topological Transformations in Chalcogenide Glasses" ***Solid State Commun*** **. 62: 101.**